*Journal of Applied Mechanics and Technical Physics, Vol. 44, No. 2, pp. 243–248, 2003*

# HEATING OF A COMPRESSIBLE LIQUID BY A CONSTANT HEAT FLUX

**G. V. Belyakov**[1] **and A. A. Charakhch'yan**[2]

UDC 537.84

*Several variants of the problem of heating a compressible liquid by a time-independent heat flux are numerically studied. It is shown that, after a certain time, the pressure everywhere behind the shock wave differs only little from some constant value. Approximate analytical formulas are obtained, which demonstrate independence of pressure of thermal conductivity and some other features of the relation between the pressure and the heat-flux intensity. Several examples are given, which confirm the adequacy of formulas to numerical solutions of the problem.*

**Key words:** *unsteady flows, compressible liquid, heat wave, shock wave, friction.*

**Introduction.** The one-dimensional problem of substance heating, posed for the heat-conduction equation without substance motion, has been well studied. This problem admits a self-similar statement for a broad class of boundary conditions and temperature dependences of thermal conductivity [1]. The problem with substance motion has been studied less extensively; here, only one self-similar solution for a particular boundary condition and thermal conductivity–temperature relation is known [2]. In [2], the distributions of propagation velocities of heat and shock waves were qualitatively compared. Presently, it is an easy matter to numerically solve the problem for given values of parameters. This, however, does not cancel the importance of analytical formulas, which allow an explicit representation of flow characteristics on problem parameters.

In the present study, we examine an important particular case of substance heating by a time-independent heat flux, which admits an analytical formula for one of the main characteristics of the flow. The interest in this problem is related to modeling of substance heating by friction, which will probably make it possible to explain specific features of one experiment on shock compression of an aluminum plate on a wedge. That is why the main example used to test the accuracy of the derived formula is somewhat exotic. We consider high-pressure aluminum melt that arises behind the front of an attached shock wave when the plate undergoes jetless compression with a 4-km/sec velocity (see [3]). We use tabulated broad-range equation-of-state data for aluminum reported in [4]. In addition, the formula is tested with the perfect-gas equation-of-state problem. For definiteness, parameters close to those of air are used.

**Statement of the Problem. Approximate Formula.** A plane one-dimensional flow of a compressible heat-conducting liquid is governed by the equations

$$\frac{d\rho}{dt} + \rho\,\frac{\partial u}{\partial x} = 0, \quad \rho\,\frac{du}{dt} + \frac{\partial p}{\partial x} = 0, \quad \rho\,\frac{d(\varepsilon + u^2/2)}{dt} + \frac{\partial (pu)}{\partial x} = \frac{\partial}{\partial x}\,æ\,\frac{\partial T}{\partial x}, \tag{1}$$

where $x$ is the spatial variable, $t$ is the time, $u$ is the velocity, $\rho$ is the density, $p$ is the pressure, $\varepsilon$ is the specific internal energy, $T(x,t)$ is the temperature, $d/dt = \partial/\partial t + u\partial/\partial x$ is the Lagrangian time derivative, and $æ = æ(\rho, T)$ is the thermal conductivity. Equations (1) are closed by the equations of state $p = p(\rho, T)$ and $\varepsilon = \varepsilon(\rho, T)$. The liquid occupies the half-space $0 \leqslant x < \infty$. At the time $t = 0$, the liquid is stationary, and the thermodynamic variables are constant: $\rho = \rho_0$, $T = T_0$, $p = p_0 = p(\rho_0, T_0)$, and $\varepsilon = \varepsilon_0 = \varepsilon(\rho_0, T_0)$. At the boundary $x = 0$, the symmetry condition $u = 0$ is posed and a constant heat flux $q$ is specified:

$$-æ\,\frac{\partial T}{\partial x}(0,t) = q. \tag{2}$$

---

[1] Institute of Geosphere Dynamics, Russian Academy of Sciences, Moscow 119334; [2] Dorodnitsyn Computing Center, Russian Academy of Sciences, Moscow 119991. Translated from Prikladnaya Mekhanika i Tekhnicheskaya Fizika, Vol. 44, No. 2, pp. 109–115, March–April, 2003. Original article submitted June 13, 2002.

Setting $u \equiv 0$ and $\rho \equiv \rho_0$ in the last equation of system (1), we obtain the heat-conduction equation

$$\rho_0 C_v \frac{\partial T}{\partial t} = \frac{\partial}{\partial x}\, æ \frac{\partial T}{\partial x} \qquad \Big(C_v = \frac{\partial \varepsilon}{\partial T}\Big). \tag{3}$$

We will call problem (3), (2) with the initial condition $T(x,0) = T_0$ the thermal problem. It is of interest to find its solution over a finite time interval $0 \leqslant t \leqslant t_*$. Assuming the coefficients $C_v$ and æ in Eq. (3) to be almost unchanged in this interval, we replace them with their constant values $C_{v0} = \partial\varepsilon(\rho_0, T_0)/\partial T$ and $æ_0 = æ(\rho_0, T_0)$. This problems admits the well-known self-similar statement [1]. Its solution has the form

$$T_h(x,t) = T_0 + \sqrt{t} A \Big[\exp(-\eta^2) - 2\eta \int\limits_{\eta}^{\infty} \exp(-\beta^2)\, d\beta\Big],$$

$$A = 2q\sqrt{\chi}/(æ_0\sqrt{\pi}\,), \quad \eta = x/(2\sqrt{\chi t}\,), \quad \chi = æ_0/(C_{v0}\rho_0). \tag{4}$$

Here $\eta$ is the self-similar variable and $\chi$ is the thermal diffusivity.

Following [2], we introduce the heat-wave velocity $\dot{x}_h$ and the shock-wave velocity $D$. Using the approximate solution of the thermal problem (4), we define the velocity $\dot{x}_h$ as the velocity of a point with a fixed self-similar variable $\eta = \eta_0$:

$$\dot{x}_h = \eta_0 \sqrt{\chi/t}. \tag{5}$$

Since $\dot{x}_h \to \infty$ as $t \to 0$ and $\dot{x}_h \to 0$ as $t \to \infty$, the condition $\dot{x}_h = D$ defines a certain time $t_*$. We assume that, from the time $t_*$ on, the shock wave leaves the heat wave behind and propagates in an undisturbed liquid. We perform the change of variables $D = \mathrm{M}c_0$ (M is the shock-wave Mach number and $c_0$ is the velocity of sound in the undisturbed liquid); then, by virtue of Eq. (5), we have

$$\sqrt{t_*} = \eta_0\sqrt{\chi}/(\mathrm{M}c_0). \tag{6}$$

An analysis of the calculations results presented below shows that the solution of problem (1), (2) possesses the following property. After the shock wave is established, the pressure everywhere behind its front differs only little from a characteristic pressure $p_*$, which is independent of $x$ and $t$. In particular, this means that the shock-wave velocity $D$ and the parameters immediately behind the shock-wave front, which can be uniquely determined from the pressure behind the front, only weakly depend on $t$. A substantial difference from the work [2], in which the dependence $D(t)$ was assumed to be the same as the time dependence of the interface temperature, i.e., $D \sim \sqrt{t}$, deserves mentioning. Another important consequence of the weak time dependence of pressure consists in the fact that, as the interface temperature increases, it closely follows the isobar $p = p_*$. Hence, if the pressure $p_*$ is known, it is possible to estimate the temperature of vaporization beginning from the intersection point of the isobar and the vaporization curve in the plane of thermodynamic variables.

To find $p_*$, we use the following two assumptions. First, we assume the interface temperature $T(0,t)$ to differ little from $T_h(0,t)$ till the time $t_*$. Substituting (6) into (4), we obtain

$$T_* = T_h(0, t_*) = T_0 + \frac{2q\eta_0}{\sqrt{\pi}\rho_0 C_{v0} c_0 \mathrm{M}(p_*)}. \tag{7}$$

The dependence $\mathrm{M}(p_*)$ is determined by the shock adiabat for the wave, that propagates in the undisturbed liquid, with the pressure behind its front equal to $p_*$. Second, we neglect the difference between the density at the interface at the time $t_*$ and the initial density $\rho_0$, which allows us to define $p_*$ by the formula

$$p_* = p(\rho_0, T_*), \tag{8}$$

which, together with (7), yields an algebraic equation for $p_*$.

Formulas (7) and (8) allow two important conclusions to be drawn concerning the manner in which the pressure $p_*$ depends on problem parameters:

1) $p_*$ is independent of the thermal conductivity $æ_0$, although the solution of problem (1), (2) and, in particular, the time $t_*$ substantially depend on æ;

2) $p_*$ increases with increasing $q$.

For weak shock waves ($\mathrm{M} \approx 1$), the temperature increment is $(T_* - T_0) \sim q$, which gives $(p_* - p_0) \sim q$ for the perfect-gas equation of state. For strong shock waves, we have $\mathrm{M}(p_*) \sim \sqrt{p_*}$. Assuming that $T_* \gg T_0$, we obtain $p_* \sim q^{2/3}$ for the perfect-gas equation of state.

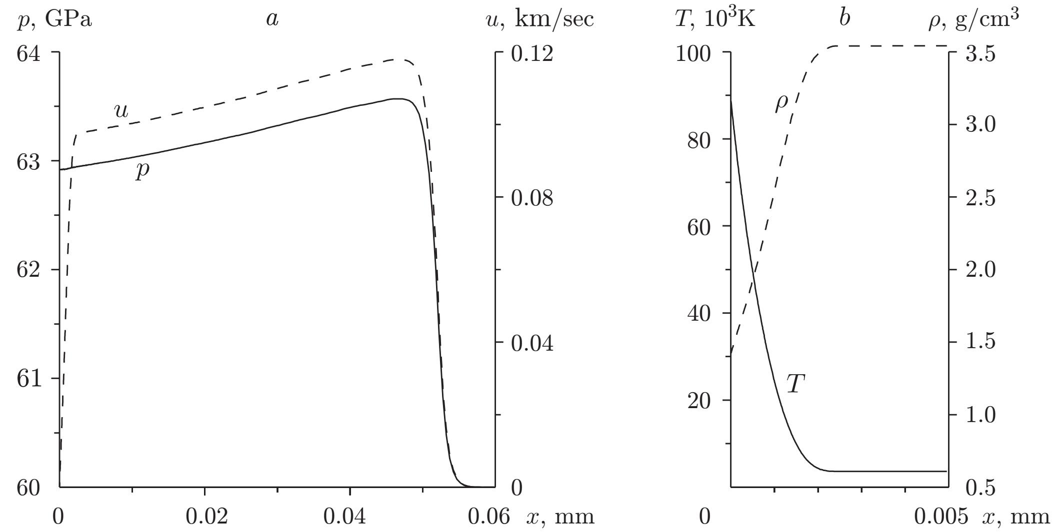

Fig. 1. Distributions of $p$ and $u$ (a) and $T$ and $\rho$ (b) at the time $t = 6$ nsec for aluminum ($q = 3$ GW/cm$^2$).

TABLE 1

| $q$, GW/cm$^2$ | $p_*$, GPa | $\bar{p}_b$, GPa | $\bar{p}_{b10}$, GPa | $\bar{p}_s$, GPa | $\bar{p}_{s10}$, GPa | $T_v$, $10^3$ K | $T_{v*}$, $10^3$ K | M($p_*$) |
|---|---|---|---|---|---|---|---|---|
| 3 | 63.2 | 62.8 | 63.5 | 63.5 | 63.6 | 141 | 141 | 1.01 |
| 30 | 82.3 | 81.9 | 81.9 | 88.1 | 88.2 | 159 | 161 | 1.07 |
| 90 | 115 | 111 | 112 | 125 | 126 | 184 | 189 | 1.20 |

**Comparison of Formulas (7) and (8) with Numerical Calculations of Problem (1), (2).** Below, we present the calculation data for problem (1), (2) obtained to test the accuracy of formulas (7) and (8). Here, the matter of adequacy of mathematical models to actual physical processes is left aside. Everywhere, if not stated otherwise, the numerical coefficient in (7) is $\eta_0 = 1$.

We consider heating of liquid aluminum with the initial data $p_0 = 60$ GPa, $\rho_0 = 3.5$ g/cm$^3$, and $T_0 \approx 3600$ K. The heat flux $q$ varies from 3 to 90 GW/cm$^2$. (The choice of the maximum value of $q$ is motivated by the restricted volume of available tabulated equation-of-state data for aluminum.) For $T \leqslant 10^5$ K, for the thermal conductivity of aluminum, we use the model [5] of electrical conductivity based on some experimental data and the Wiedemann–Franz law (see [6]). The thermal conductivity at higher temperatures ($T > 10^5$ K) is calculated by the formula $\text{æ}(\rho, T) = \text{æ}(\rho, T_c)(T/T_c)^{5/2}$, where $T_c = 10^5$ K.

Figure 1 shows the distributions of $p$, $u$, $\rho$, and $T$ along the $x$ axis for $q = 3$ GW/cm$^2$ at $t = 6$ nsec. The coordinate $x_s \approx 0.06$ mm corresponds to the position of the shock-wave front, where the largest pressure difference is observed. The heat wave, at whose front the greatest changes in temperature and density occur, have passed a much shorter distance ($x_h \approx 0.002$ mm). The pressure in the heat-wave region is almost uniform, and it gradually increases in the region between the heat and shock waves.

Figure 2 shows the time dependences of the interface pressure $p_b(t) = p(0, t)$ and the pressure behind the shock-wave front $p_s(t)$ gained for the same conditions. Initially, both pressures increase to an almost identical value and then slowly decrease. The function $p_s(t)$ decreases much more slowly than $p_b(t)$. The same figure shows the pressure $p_*$ calculated by formulas (7) and (8). The pressure $p_*$ is seen to be a good approximation for $p_s(t)$, representing a mean value of $p_b(t)$.

Table 1 compares the calculation results for problem (1), (2) with $p_*$ and with the vaporization temperature $T_{v*}$ calculated as the intersection point of the isobar $p = p_*$ and the vaporization curve found with an accuracy to the step of the tabulated equation-of-state data used. The same approximate vaporization curve was used to determine the temperature of vaporization beginning $T_v$ in the solution of problem (1), (2).

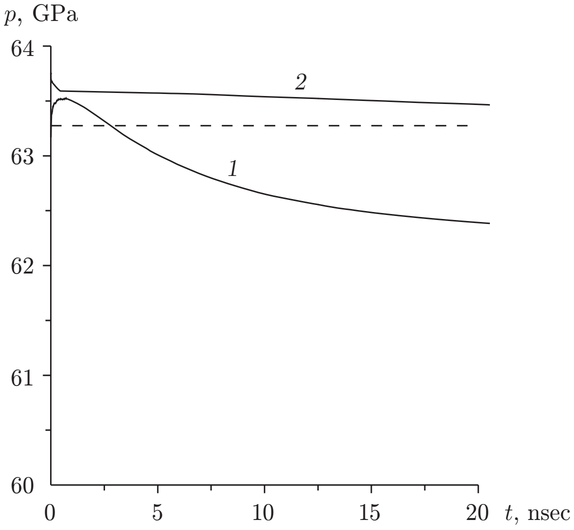

Fig. 2. Time dependences of interface pressure and pressure behind the shock-wave front: 1) $p_b$, 2) $p_s$; the dashed curve shows the pressure $p_*$ calculated by formulas (7) and (8).

To quantitatively compare the pressure $p_*$ with the functions $p_b(t)$ and $p_s(t)$, these functions were averaged by the formula

$$\bar{p} = \frac{1}{t_{\max} - t_0} \int\limits_{t_0}^{t_{\max}} p(t)\, dt,$$

where $t_{\max}$ is the maximum time till which the evolution of the system was traced and $t_0$ is the time at which the dependence $p(t)$ attains its maximum. The resultant quantities are denoted as $\bar{p}_b$ and $\bar{p}_s$ (see Table 1). The designations $\bar{p}_{b10}$ and $\bar{p}_{s10}$ are used for the respective mean values for problem (1), (2) with tenfold increased thermal conductivity æ. Almost for all variants, the calculations were conducted till the vaporization started. The only exception is the variant with $q = 3$ GW/cm$^2$ and tenfold increased æ, in which case the calculation till vaporization beginning would require a much greater number of time steps. Nevertheless, the time $t_{\max}$ in this case was almost the same as in the case without increased æ.

First of all, it should be noted that the pressure obtained from the solution of problem (1), (2) is almost independent of thermal conductivity, which is in line with formulas (7) and (8). Simultaneously, other functions essentially depends on æ. For instance, the interface temperature at the time $t = 6$ nsec (see Fig. 1) is $T(0,t) \approx 9 \cdot 10^4$ K. For the tenfold increased æ, the calculations yield $T(0,t) \approx 3 \cdot 10^4$ K.

The values predicted by formulas (7) and (8) agree well with the data obtained by numerical calculations. As $q$ increases by 30 times and $p_*$ by a factor of two, the mean values of pressure deviate from $p_*$ within 10%; for the vaporization temperatures, this deviation is within 3%.

As is evident from the last column of Table 1, the variants of problem (1), (2) described above correspond to the case of weak shock waves. In the case of strong shock waves, the accuracy of formulas (7) and (8) was tested on problem (1), (2) with the perfect-gas equation of state $\varepsilon = p/(\rho(\gamma - 1))$, where $p = R\rho T$ (for definiteness, the constants $\gamma$ and $R$ were taken to correspond to deionized air). The thermal conductivity was assumed to be constant, $æ = æ_0 = 4.2 \cdot 10^{-4}$ W/(cm $\cdot$ K) or $æ = 10æ_0$, where $æ_0$ is close to the corresponding value for cool air. The initial data are $p_0 = 1$ atm and $\rho_0 = 1.205 \cdot 10^{-3}$ g/cm$^3$.

Figure 3 shows the dependences $p_s(t)$ and $p_s(t)$ for the variant with $q = 30$ MW/cm$^2$. Unlike the case of aluminum, both functions are monotonically increasing and close to each other. This means that the pressure everywhere behind the shock-wave front is almost independent of $x$. As $t \to \infty$, both functions tend to a certain value $p_\infty$. A tenfold increase in æ affects the time dependence of pressure, but the value of $p_\infty$ remains unchanged, similarly to the case of aluminum and in line with formulas (7) and (8).

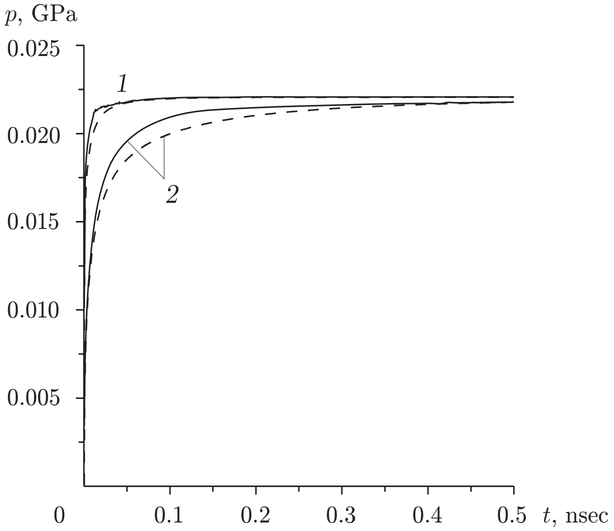

Fig. 3. Time dependence of interface pressure and pressure behind the shock-wave front for air ($q = 30$ MW/cm$^2$): the solid and dashed curves refer to $p_b$ and $p_s$, respectively, for $æ = æ_0$ (1) and $10æ_0$ (2).

TABLE 2

| Variant No. | $q$, MW/cm$^2$ | $p_*$, MPa | $p_\infty$, MPa | M($p_*$) |
|---|---|---|---|---|
| 1 | 30 | 26.5 | 22.06 | 15.0 |
| 2 | 300 | 122.6 | 102.1 | 32.4 |

Table 2 contains the values of $p_\infty$ and $p_*$ for two values of $q$ differing tenfold from each other. The difference between $p_\infty$ and $p_*$ does not exceed 20%. The accuracy provided by formulas (7) and (8) seems to be satisfactory since, for various values of $q$, the pressures in Table 2 differ by a factor of 4.5. Note that formulas (7) and (8) are accurate to the numerical factor $\eta_0$. The values of $p_*$ given in Table 2 are obtained for $\eta_0 = 1$. A proper choice of $\eta_0$ makes it possible to improve the accuracy of formulas (7) and (8); this is confirmed by the example given below. If, in variant No. 1 ($q_1 = 30$ MW/cm$^2$), we choose the value of $\eta_0$ so that to make the pressure $p_*$ be coincident with $p_\infty$ within the accuracy to three decimal digits, then the pressure $p_*$ in variant No. 2 ($q_2 = 300$ MW/cm$^2$) will also coincide with $p_\infty$ within the accuracy to three decimal digits. This means that the error of formulas (7) and (8) is smaller than 1%. The relation $p_* \sim q^{2/3}$ for strong shock waves obtained above from the analysis of formulas (7) and (8) also holds within a 1% error. For the values indicated in Table 2, we have

$$(q_2/q_1)^{2/3} \approx 4.64; \qquad p_{*2}/p_{*1} \approx p_{\infty 2}/p_{\infty 1} \approx 4.63$$

(the subscripts 1 and 2 refer to the variant number in Table 2).

**Conclusions.** All of the variants of problem (1), (2) considered demonstrate good agreement between the pressures obtained from the numerical solution of the problem and the pressures calculated by formulas (7) and (8). The pressure is almost independent of thermal conductivity. The only exception is the initial time interval over which the pressure rises. As the heat flux increases, the pressure grows in value. In the case with aluminum, the error in determination of pressure is within 10%, and the error in determination of the temperature of vaporization beginning is within 3%. In the case with a perfect gas, a proper choice of the numerical coefficient $\eta_0$ makes it possible to reduce the error of formulas (7) and (8) to less than 1%.

In addition to the problem with a time-independent heat flux, we also considered the problem of heating of melted aluminum with a heat flux varying in proportion to the interface pressure:

$$q = q_0 p_b(t)/p_0, \qquad q_0 = \text{const}.$$

The calculations showed that, in the latter problem, the pressure behaves similarly to the case with $q = \text{const}$. The characteristic pressure $p_*$ can be found from formulas (7) and (8) with $q$ replaced by the dependence $\bar{q}(p_*)$, which determines an appropriate mean value of $q$ from the interval $p_0 \leqslant p_b \leqslant p_*$. The dependence $\bar{q} = q_0(0.25 + 0.75 p_*/p_0)$

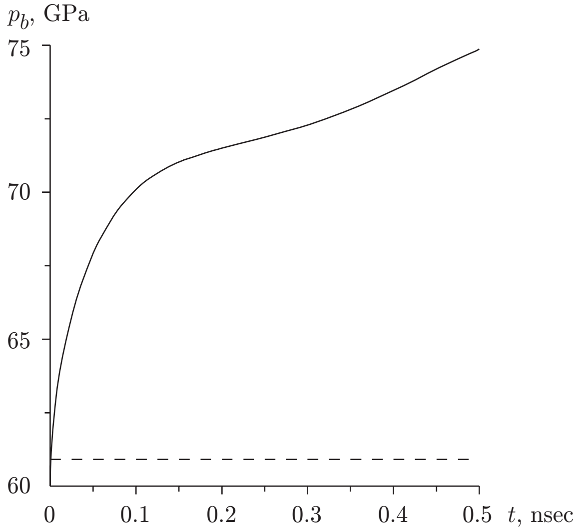

Fig. 4. Time dependence of interface pressure (solid curve) and $p_*$ (dashed curve) for the problem with the boundary condition (9).

ensured a lower than 1 K error in determining the temperature of vaporization beginning $T_v$ by formulas (7) and (8) for $q_0 = 30$ and 90 GW/cm$^2$. It should be emphasized that the high accuracy in determination of $T_v$ by no means implies that the pressures $p_*$ and $p_0$ lie close together, since $p_* \approx 90$ GPa for the first value and $p_* \approx 160$ GPa for the second value of $q_0$, which is higher than $p_0$ approximately by a factor of 1.5 and 2.5, respectively.

Finally, the reader should be forewarned against formal using of the derivation methods of formulas (7) and (8) for problems with boundary conditions other than (2). As an example, we consider the problem with the boundary condition

$$T(0,t) = T_0 + \beta t \qquad (\beta = \text{const}). \tag{9}$$

The solution of the corresponding thermal problem with constant coefficients is a function of the same self-similar variable on which solution (4) depends. Hence, formulas (5) and (6) remain unchanged. Inserting $t_*$ from Eq. (6) into Eq. (9), we obtain $T_*$ and then, as previously, use formula (8) to find $p_*$. Figure 4 shows the value of $p_*$ thus obtained and the interface pressure $p_b(t)$ for $\beta \approx 4.3 \cdot 10^{14}$ K/sec. It is seen that, in the case of interest, the pressure $p_*$ bears no relation to the function $p_b(t)$.

The authors are grateful to I. V. Lomonosov and K. V. Khishchenko for providing them with tabulated equation-of-state data for aluminum.

This work was partially supported by the Russian Foundation for Fundamental Research (Grant No. 00-01-00551).

## REFERENCES

1. G. I. Barenblatt, “Some types of unsteady gas and liquid flows in porous media,” *Prikl. Mat. Mekh.*, **16**, No. 1, 67–78 (1952).
2. Ya. B. Zel’dovich and Yu. P. Raiser, *Physics of Shock Waves and High-Temperature Hydrodynamic Phenomena* [in Russian], Nauka, Moscow (1966).
3. A. A. Charakhch’yan, ”Shock compression of a plate on a wedge-shaped target,” *J. Appl. Mech. Tech. Phys.*, **42**, No. 1, 14–20 (2001).
4. A. V. Bushman, G. I. Kanel’, A. L. Ni, and V. E. Fortov, *Thermal Physics and Dynamics of Intense Pulsed Actions* [in Russian], Inst. of Chem. Phys., USSR Acad. of Sci., Chernogolovka (1988).
5. A. A. Charakhch’yan, “Numerical study of the spontaneous electromagnetic field generated by circular cumulative jets in conical targets,” *Fiz. Plazmy*, **24**, No. 4, 349–355 (1998).
6. V. V. Ermakov and N. N. Kalitkin, “Electron transport in superdense nondegenerated plasma,” Preprint No. 26, Inst. of Applied Mathematics, USSR Acad. of Sci., Moscow (1977).